陈梅, 田作林, 张聪, 等. 拉萨地块松多超高压变质带含石榴石云母石英片岩的变质演化相平衡模拟[J]. 中国地质, 2015, 42(5): 1572−1587.
Chen Mei, Tian Zuolin, Zhang Cong, et al. Phase equilibrium modeling for metamorphic evolution of garnet-bearing mica-quartz schist in Sumdo UHP metamorphic belt, Lhasa Block[J]. Geology in China, 2015, 42(5): 1572−1587(in Chinese with English abstract).

拉萨地块松多超高压变质带含石榴石云母石英片岩的变质演化相平衡模拟

陈 梅[1,2] 田作林[1] 张 聪[1] 杨经绥[1] 黄 杰[1,2]

(1. 中国地质科学院地质研究所,大陆构造与动力学国家重点实验室,北京 100037;
2. 中国地质大学地球科学与资源学院,北京 100083;)

提要:拉萨地块松多超高压变质带含石榴石白云母石英片岩为榴辉岩的围岩,岩石的矿物组合为石榴石、白云母、钠长石、绿泥石、石英及少量金红石、榍石。石榴石具有明显的成分环带,从核部到幔部Xprp= [Mg/(Mg+Fe+Mn+Ca)]缓慢升高,Xsps= [Mn/(Mg+Fe+Mn+Ca)]逐渐降低,表明石榴石从核部到幔部的成分记录了温度逐渐升高的进变质过程;幔部到边部,Xprp= [Mg/(Mg+Fe+Mn+Ca)]略微降低,Xgrs= [Ca/(Mg+Fe+Mn+Ca)]明显升高,Xsps= [Mn/(Mg+Fe+Mn+Ca)]先升高后降低,表明石榴石边部成分受到了退变质作用改造,呈现扩散环带的特征。利用Thermocalc变质相平衡计算软件在MnNCKFMASHO体系下计算出含石榴石云母石英片岩的*P*−*T*、*P*−M(H_2O)视剖面图,结合石榴石镁铝榴石等值线、钙铝榴石等值线及饱和水含量等值线限定出含石榴石云母石英片岩的峰期变质条件为约27×10^5 kPa,523/580℃,对应的峰期矿物组合为(g−Jd−Cr−Law(+Phn+q/Coe+H_2O)。石榴石核部到幔部成分记录了主要的进变质演化,结合饱和水等值线的变化,判断进变质阶段为升温升压的冷俯冲过程,岩石经历了蓝片岩相至榴辉岩相的变质演化;*P*−M (H_2O)视剖面图及饱和水等值线反映了岩石在减压中的流体行为,通过其变化特征可以确定岩石在峰期之后先经历近等温降压的早期退变质过程,晚期降温降压的退变轨迹则由石榴石边部成分所确定,此过程中,岩石发生了角闪岩相至绿帘角闪岩相变质,并在后期经历了绿片岩相变质叠加。近等温降压的退变质过程反映了快速抬升的构造运动过程,早期硬玉转变为钠长石可能发生在这个阶段。对比含石榴石云母石英片岩与榴辉岩的*P*−*T*轨迹,峰期变质温压及变质演化特征,提出含石榴石云母石英片岩曾经历过高压变质,结合野外相互伴生的地质关系,认为该片岩与榴辉岩经历了相同或者相似的俯冲折返过程。

关 键 词:拉萨地体;松多超高压变质带;含石榴石云母石英片岩;相平衡模拟;变质演化
中图分类号: P588.34+4 **文献标志码**: A **文章编号**: 1000−3657(2015)05−1572−16

Phase equilibrium modeling for metamorphic evolution of garnet−bearing mica−quartz schist in Sumdo UHP metamorphic belt, Lhasa Block

收稿日期:2015−06−18;**改回日期**:2015−08−19
基金项目:国家自然科学基金项目(41202034)、中国地质调查局面上项目(12120115026801,12120114061501)及中国地质科学院地质研究所基本科研业务费(J1518)资助。
作者简介:陈梅,女,1991年生,硕士生,从事变质岩岩石学研究工作;E−mail:634728280@qq.com。
通讯作者:张聪,男,1983年生,副研究员,从事变质地质学及超高压岩石学工作;E−mail: congzhang@pku.edu.cn。

CHEN Mei[1,2], TIAN Zuo-lin[1], ZHANG Cong[1], YANG Jing-sui[1], HUANG Jie[1,2]

(1.*State Key Laboratory for Continental Tectonics and Dynamics*, *Institute of Geology, Chinese Academy of Geological Sciences, Beijing* 100037, *China;* 2. *School of Earth Science and Mineral Resources*, *China University of Geosciences*, *Beijing* 100083, *China*)

Abstract: The garnet-bearing mica-quartz schist of Sumdo UHP belt in Lhasa block occurs as country rocks of eclogite, and is mainly composed of garnet, muscovite, albite, chlorite, quartz and minor rutile and sphene. Garnet displays an obvious compositional zonation where Xprp increases from the core to the mantle and then decreases in the rim, whereas Xsps decreases gradually from the core to mantle, with the trend of declining following rising in the rim, indicating that garnet composition profiles from core to mantle have preserved the prograde growth zoning and were partially reset during retrogression. The model system MnNCKFMASHO was chosen to calculate *P*-*T* and P-M(H_2O) pseudosections of the garnet-bearing mica-quartz schist. Garnet isopleth thermobarometry involved plotting compositional isopleths of garnet as contours on a *P*-*T* pseudosection, with the combination of contours of saturated H_2O content, thus obtaining estimated peak *P*-*T* conditions of 27 kbar, 523/580 ℃ and peak mineral assemblages of g-jd-cr-law (+phn +q/coe+H_2O). The compositional profile of garnet from the core to the mantle and contouring of the H_2O content saturated indicate that prograde metamorphic evolution represents a cold subduction stage with heating with the increasing pressure, and the rocks experienced blueschist- facies to eclogite- facies metamorphism during this stage. *P*-M(H_2O) pseudosections and isopleth of saturated H_2O content could be used to assess evolution of mineral assemblages in terms of changes in water content during decompression, which shows that garnet-bearing mica quartz schist experienced an early isothermal decompression process and was then followed by a cooling with decompression evolution during the late stage. Amphibolite- facies to epidote-amphibolite- facies metamorphism occurred during early stage and was followed by greenschist- facies metamorphism. The isothermal decompression of garnet- bearing mica- quartz schist probably represents a fast tectonic exhumation. Albite was likely to replace early jadeite at this stage. A comparison with the *P*-*T* path and contact relationship in the field of garnet-bearing mica-quartz schist and eclogite shows evidently that garnet-bearing mica-quartz schist and the eclogite it hosted experienced similar subduction and exhumation processes.

Key words:Lhasa block; Sumdo UHP metamorphic belt; garnet- bearing mica quartz schist; phase equilibrium modeling; metamorphic evolution

About the first author: CHEN Mei, female, born in 1991, master candidate, majors in metamorphic petrology; E- mail: 634728280@qq.com.

About the corresponding author: ZHANG Cong, male, born in 1983, associate professor, mainly engages in the study of metamorphic geology and UHP petrology; E-mail: congzhang@pku.edu.cn.

高压-超高压变质岩常产于汇聚板块边界,它记录了地表岩石俯冲达近地幔-地幔深度发生高压-超高压变质作用及折返过程中的一系列地球动力学信息[1-10]。高压-超高压榴辉岩是大洋俯冲和大陆碰撞的重要标志,常与冷俯冲型低温高压蓝片岩伴生,或呈透镜状或层状产于变质泥质岩、长英质片岩、片麻岩等岩石中[3,11-13]。有关榴辉岩与其围岩伴生关系的探讨一直存在"原地"和"外来"的争议,Smith 1988[8]提出榴辉岩可通过构造侵位被围岩包裹的"外来"模式[8],此过程中榴辉岩与围岩经历了完全不同的变质演化;后来有研究发现,榴辉岩可以与围岩同时俯冲折返,经历相同的变质演化过程,二者为"原地"关系[14-17],如西南天山、柴北缘及大别山HP-UHP变质带,此时榴辉岩与围岩中的超高压矿物柯石英等可作为二者同时俯冲折返的岩相学证据。新的研究表明,长英质及泥质岩石中含有较多的含水矿物相,抗外界改造的能力较弱,寄于其中的高压矿物容易受到后期改造而难以保存下来[18-19],仅以围岩中缺少高压指示性矿物及结构特征这一证据并不能说明其与寄主榴辉岩的变质演化关系。因此,有必要对榴辉岩的围岩展开深入研究,以期找到新的证据来解释二者的关系,这对于进一步揭示榴辉岩及其围岩在俯冲折返和造山带演化过程中的地质作用具有重要意义。此前,陆续有学者开展了对榴辉岩围岩-变泥质岩、长英质片岩、片麻岩的岩石学研究[19-25],研究着眼于此类岩

石的岩相学、矿物化学特征，并在此基础上进行详细的变质演化讨论，再结合同位素年代学证据，进而限定片岩、片麻岩的*P*–*T*轨迹及其与榴辉岩的伴生关系，为探讨榴辉岩的形成及演化过程提供理论依据。

拉萨地块松多榴辉岩带自发现以来就引起了广泛关注[26–30]。前人研究提出将拉萨地块通过狮泉河—纳木错混杂带和洛巴堆—米拉山断裂一分为三的构造格局[31–33]，但随着松多榴辉岩带的发现，将其两分的建议逐渐兴起，认为在拉萨地块中部可能存在一条新的板块缝合带[28–30]。随着研究工作的陆续展开，已发表的岩石地球化学研究表明，榴辉岩的原岩可能为MORB型的大洋玄武岩[34–36]；锆石U–Pb年龄约为260 Ma，初步确定该榴辉岩的变质时代为二叠纪[26–30]；此外，为揭示榴辉岩的变质演化历史，前人对其变质过程及峰期温压条件进行了计算和模拟，分别得到(26~27)×10^5 kPa，650~750℃[28]；(33~39)×10^5 kPa, 760~800℃[37]；(34~38)×10^5 kPa，753~790℃[34]；30×10^5 kPa,610℃[38]。但前人对松多榴辉岩围岩的研究很少，杨德明等(2005)[39]得到松多群的主期变质温压条件为(9.3~11.5)×10^5 kPa, 500~553℃；Li(2009)[40]利用白云母^{40}Ar–^{39}Ar测年法对松多群韧性剪切带的绿片岩进行研究得出了220~230 Ma的变质年龄，并通过白云母的封闭温度限定，认为松多群岩石经历过中压角闪岩相变质。对于温压条件的研究，前人的工作主要是利用矿物对温压计来限定变质温压条件，有研究证明，利用传统的地质温压计限定含高压矿物的岩石形成的温压条件存在一定的局限性[18,41–45]。为找到行之有效的方法解决这一难题，热力学相平衡正演模拟方法在实践尝试中应运而生，将热力学理论应用于镁铁质、长英质及泥质变质岩等岩石中，利用*P*–*T*视剖面图限定其变质温压条件，成为许多学者所认可的一种模拟变质演化过程的理想方式[25, 45–46]。

本文对松多地区榴辉岩的围岩含石榴石云母石英片岩进行详细的岩石学、矿物化学研究，并利用Thermalcalc相平衡模拟软件，在MnO–Na_2O–CaO–K_2O–FeO–MgO–Al_2O_3–SiO_2–H_2O–O(Fe_2O_3)(MnNCKFMASHO)体系进行相平衡模拟，确定该类岩石变质演化的*P*–*T*轨迹，并与榴辉岩变质演化过程相比较，限定含石榴石云母石英片岩与榴辉岩的关系，进而探讨其所代表的地质意义。

1 区域地质背景

拉萨地块作为青藏高原造山格局的重要组成部分，在青藏高原形成和演化中具有重要地位。从地理位置来看，它地处西藏南部，南北宽约300 km，东西向延展近2000 km。从大地构造背景来看，它位于印度河—雅鲁藏布江缝合带之北，班公湖—怒江缝合带以南(图1–b)。前人研究表明，拉萨地块以发育前寒武纪变质结晶基底、古—中生代海相沉积地层、岛弧型火山岩以及中—新生代侵入体为主要特征[31–33, 47–54]，其中，变质基底为念青唐古拉岩群，出露于拉萨地块东部的波密—察隅和中部的念青唐古拉山一带，岩石类型主要为含石榴石黑云斜长片麻岩、黑云二长片麻岩、斜长角闪片岩、大理岩、石英岩及花岗片麻岩等，传统意义上认为它属于前震旦纪底层，但那木错西缘念青唐古拉岩群中最新获得的锆石年龄为748~787 Ma，它代表该岩群中正片麻岩的原岩年龄[55]，岩石在后期又经历了718 Ma的中压角闪岩相变质作用[56]和650 Ma的高压麻粒岩相变质作用[57]；Dong(2011)[58]对羊八井附近角闪岩进行研究，给出了213~225 Ma的锆石U–Pb年龄，并得出该处念青唐古拉群的变质时代为三叠纪。拉萨地块北部拉萨河以东一带还发育低绿片岩–低角闪岩相变质岩系，属于前奥陶纪地层[59]，2004年新版的《青藏高原地质图》将其统归为石炭系—二叠系[60]，为最近发现的拉萨地块松多高压带榴辉岩的围岩[28]。

松多榴辉岩产于拉萨地块中东部，距拉萨市近200 km处的工布江达县松多乡一带(图1–a)，呈近东西向展布，延伸规模在100 km以上[28, 61–62]。其围岩主要为绿帘角闪岩、含石榴石石英云母片岩、含石榴石云母石英片岩、石榴石绢云母千枚岩、泥质板岩等。野外观察到榴辉岩呈厚层状产出，与绿帘角闪岩相接触。岩性从超基性岩→绿帘角闪岩→榴辉岩→绿帘角闪岩→含石榴石石英云母片岩→含石榴石云母石英片岩→石英岩，颜色由深到浅依次过渡。含石榴石云母石英片岩的产出位置与榴辉岩仅相差500 m左右，据此推测未出露的部分榴辉岩可与之接触(图2–a)。关于围岩的时代，前人做过一些探讨：中国科学院青海盐湖所采用Rb–Sr

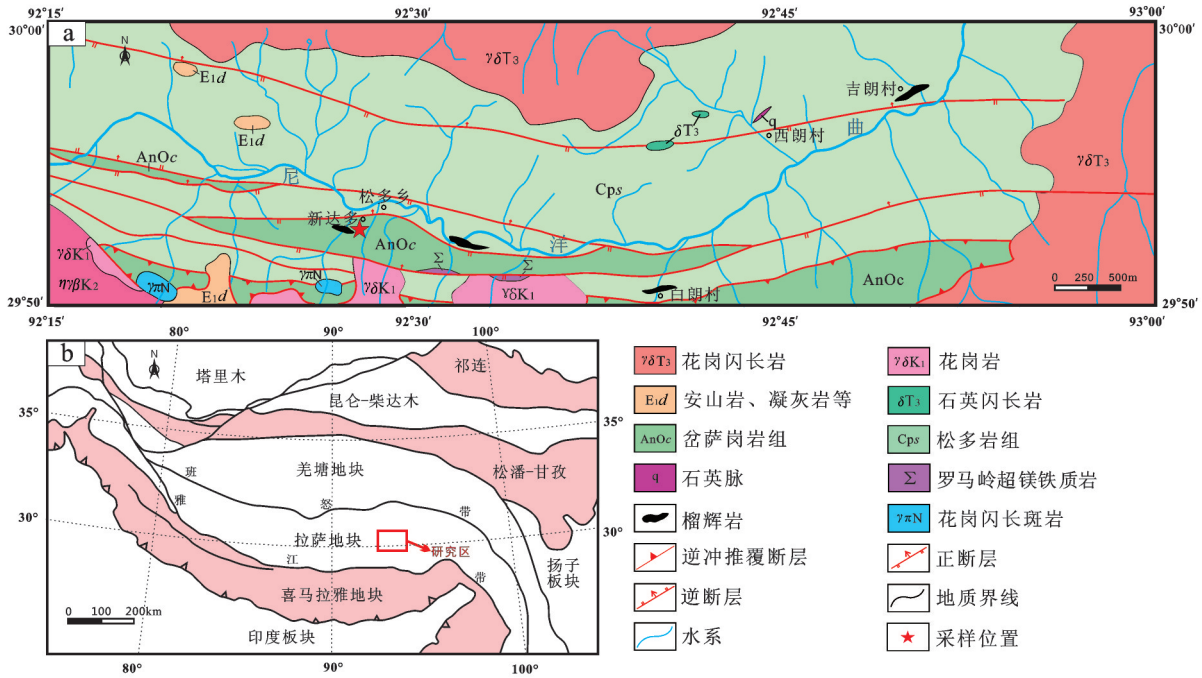

图1 拉萨地块松多地区区域地质简图

a—研究区地质图(据文献[59]修改); b—青藏高原构造单元划分简图(据文献[60])

Fig.1 Geological map of the Sumdo area in Lhasa terrane

a−Geological sketch map of the study area (after reference [59]); b−Simplified map of tectonic subdivision of the Tibetan Plateau (after reference [60])

等时线获得该带石英片岩的变质年龄为507 Ma[59];杨德明(2005)[39]认为松多群主期变质为加里东期变质作用的产物;也有研究者提出,该围岩在220~230 Ma时经历了由角闪岩相至绿帘角闪岩相的中压变质作用[40,63]。本论文主要针对含石榴石云母石英片岩的岩石学特征进行研究,采样点位置如图1−a所示,岩石的野外特征如图2−b和图2−c所示。

2 岩相学特征

岩石主要矿物组合为石榴石(5%~10%)、石英(50%~55%)、白云母(15%~20%)、钠长石(10%~15%)、绿泥石(5%)、黑云母(3%)等,并含有少量的副矿物(2%),如金红石、锆石、榍石、磷灰石等。

石榴石主要以变斑晶形式存在,粒度大小不一,粒径介于0.5~2 mm,裂隙发育。少数自形程度较好的颗粒边界平直,可见两期生长特征:核部浑圆状石榴石被边部自形石榴石包裹(图3−b)。石榴石包体以石英为主,并含有少量白云母、钠长石、金红石和磷灰石等,其中少数石英包体周围出现放射状裂纹,可能标志着早期柯石英的存在(图3−a)。多数石榴石自形程度较差,其边界通常具港湾状构造或已经完全退变呈骸晶状假象(图3−c),白云母沿骸晶边部生长并随之发生旋转,表明该岩石遭受了明显的退变质作用改造,其矿物组合可能并不能代表变质峰期矿物组合。

云母类矿物包括白云母和黑云母。薄片中可见白云母呈三种产状:(1)多数白云母呈针状或者叶状产于基质中,构成主期片理图(图3−e);(2)部分白云母包裹在钠长石中,并与之构成筛状结构(图3−d);(3)少量白云母以包体形式存在于石榴石中,或生长于石榴石“假象”的边部(图3−c)。黑云母生长于石榴石或者白云母边部,含量较少。

钠长石呈半自形粒状,颗粒较大,粒径在1~5 mm。多数周围有白云母围绕其生长,部分钠长石包裹白云母包体,构成筛状结构(图3−d),少量钠长石以包体形式存在于石榴石中(图3−f)。

绿泥石主要存在于基质中,形状不规则,部分生长于白云母边部或石榴石裂隙中(图3−a、b、d、

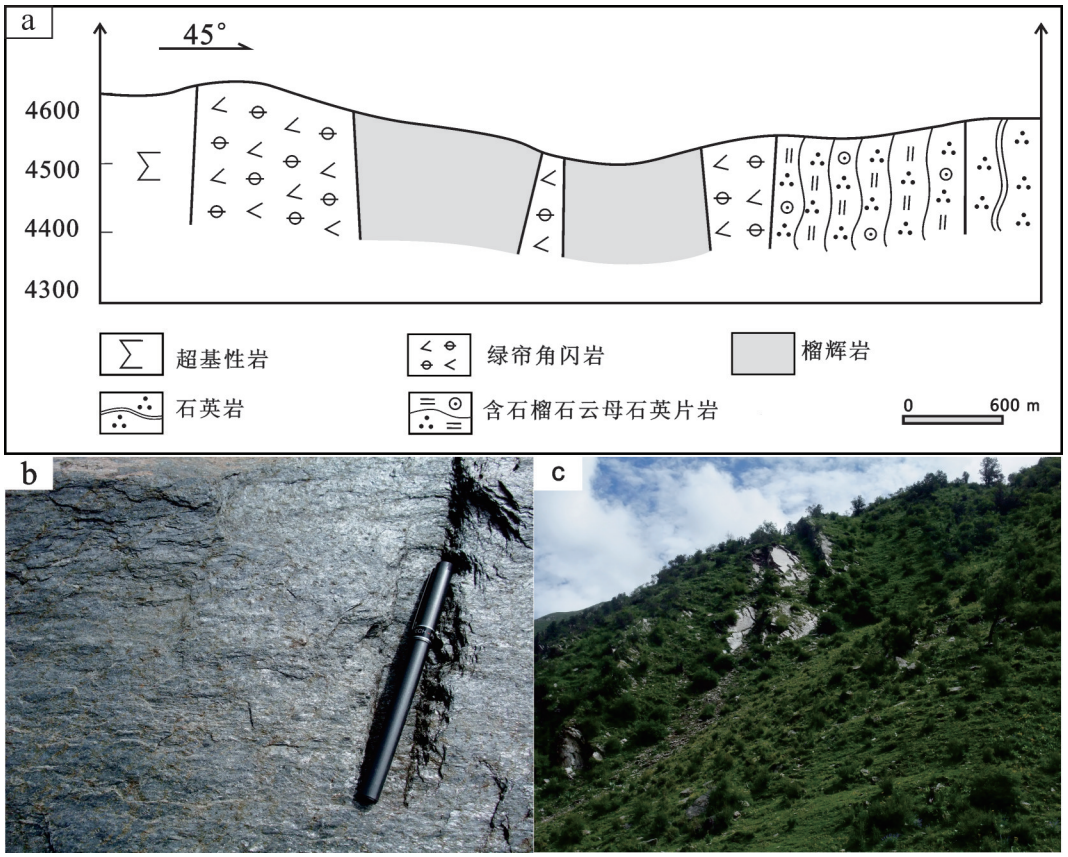

图2 松多含石榴石云母石英片岩的产状及野外照片

a—含石榴石云母石英片岩及其周围岩石的岩性剖面;b-c—含石榴石石英云母片岩的野外照片(b为岩石野外特征,c—为岩石出露产状

Fig. 2 Field attitude of Sumdo garnet-bearing mica-quartz schist

a-Geological section of the garnet-bearing mica-quartz schist and other adjacent rocks ; B and c-Field photos of garnet-bearing mica-quartz schist; b-Field features of garnet-bearing mica-quartz schist, c-Field attitude of Sumdo garnet-bearing mica-quartz schist

f)。金红石以包体形式存在于石榴石中(图3-a)。

3 矿物化学与全岩成分特征

3.1 矿物化学特征

含石榴石白云母石英片岩(13SD24)矿物电子探针分析在中国地质科学院地质研究所电子探针实验室完成,所用仪器型号为JXA-8100,测定条件为:加速电压15 kV,电流20 nA,电子束斑5 μm。具有代表性的矿物电子探针成分分析如表1。

(1) 石榴石

石榴石主要由铁铝榴石(Alm)、镁铝榴石(Prp)、钙铝榴石(Grs)和锰铝榴石(Sps)组成,其中以铁铝榴石组分为主,含量可达80%。各个组分都呈现出显著的成分环带特征(表1和图4-a),从核部到幔部,钙铝榴石和锰铝榴石组分含量逐渐降低,铁铝榴石和镁铝榴石组分含量逐渐升高,其中锰铝榴石组分所呈现出的"钟型"结构代表了进变质生长环带特征[64];从幔部到边部,钙铝榴石组分含量快速升高,锰铝榴石组分含量略有升高,铁铝榴石和镁铝榴石组分含量快速降低,锰铝榴石组分的升高和镁铝榴石组分的降低表明石榴石的边部成分受到了退变质作用改造[64]。

(2)白云母

白云母包括硅值较低的普通白云母(Si=3.18~3.26 pfu,Fe+Mg=0.21~0.35 pfu;pfu为单个分子中的离子数,下同),以及硅含量较高的多硅白云母(Si=3.34~3.49 pfu,Fe+Mg=0.40~0.44 pfu),其中保存较好的石榴石边部的白云母及钠长石中包体白云母的硅值略高于基质中的(表1,图4-b),这说明不同产状的白云母可能为不同变质作用阶段的产物。

3.2 全岩成分特征

本研究在限定温压条件时将利用Thermocalc

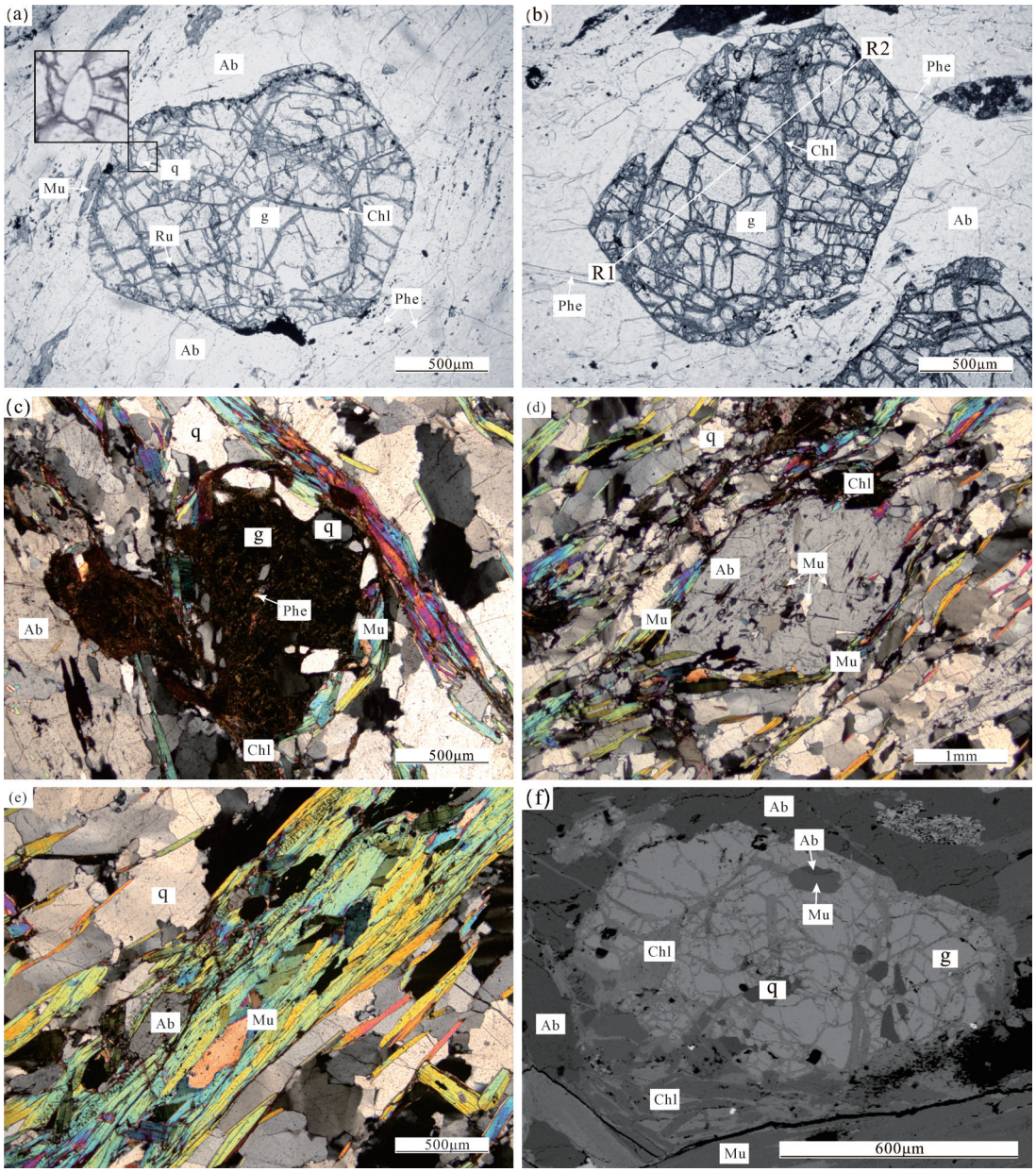

图3 松多含石榴石云母石英片岩的显微照片及背散射图像

a—石榴石(周围被钠长石包裹)中含金红石、石英包体,石英包体周围出现放射状裂纹;b—石榴石(周围被钠长石包裹)边界较平直,从R1→R2的白线指示图4-a中石榴石成分环带的位置;c—石榴石变形"假象";d—钠长石中包裹白云母,构成"筛状结构";e—构成主期片理的白云母;f—石榴石中的钠长石及白云母包体;

g—石榴石;Jd—硬玉;o—绿辉石;Chl—绿泥石);Pa—云母;Bi—黑云母;Ab—钠长石;Phe—多硅白云母;Mu—白云母;q—石英;Ru—金红石;

Fig. 3 Photomicrographs and backscattered electron image of Sumdo garnet-bearing mica-quartz schist

a-A garnet porphyroblast in albite, with inclusions of rutile and quartz, radial cracks around quartz inclusion; other opaque phases in albite comprise biotite and phengitic muscovite; b-A garnet porphyroblast in albite, the white line represents the composition profile in Fig. 4a; c-The rim of garnet porphyroblast replaced by muscovite, with the preservation of crystal shape; d-Albite with inclusions of muscovite; e-Attitude of muscovite consistent with schistosity; f-Grains of quartz, albite and muscovite in garnet

g-Garnet; Jd-Jadeite; o-Omphacite; Chl-Chlorite; Pa-Paragonite; Bi-Biotite; Ab-Albite; Phe-Phengite; Mu-Muscovite; q-Quartz; Ru-Rutile;

表1 松多含石榴石云母石英片岩(13SD24)的代表性矿物的电子探针成分分析(%)

Table 1 Electron microprobe analyses of Sumdo garnet-bearing mica-quartz schist (13SD24)(%)

Mineral	g-C	g-C	g-M	g-M	g-R	g-R	mu-R	mu	ab	ab	chl	chl
SiO_2	36.51	35.76	36.46	36.58	37.84	37.58	52.31	48.36	68.9	68.94	26.54	26.74
TiO_2	0.06	0.06	0.01	0.04	0.02	0.05	0.25	0.05	11.6	11.47	0.08	0.01
Al_2O_3	20.02	20.89	20.39	20.98	20.25	20.49	25.83	33.78	0	0.03	21.41	21.29
Cr_2O_3	0	0.05	0	0.03	0.02	0.02	0.09	0	0.08	0.1	0.04	0
Fe_2O_3	1.77	1.77	1.77	1.77	1.77	1.77	0	0	0	0	0	0
FeO	34.35	34.44	35.92	36.65	29.12	28.02	2.29	1.41	19.2	19.4	25.21	24.68
MnO	4.8	3.58	1.68	1.42	0.94	1.25	0	0	0	0.02	0.14	0.16
MgO	1.23	2.27	1.98	2.48	2.33	1.27	3.19	1.34	0.29	0.24	15.04	16.09
CaO	3	2.33	2.91	2.3	7.83	11.29	0.02	0.01	0.03	0	0.02	0.01
Na_2O	0.12	0.13	0.09	0.16	0.2	0.1	0.6	1.29	0.21	0.02	0.03	0.02
K_2O	0.03	0.03	0.03	0.03	0.03	0.04	10.43	9.63	0	0	0.01	0.01
Oxygens	12	12	12	12	12	12	11	11	8	8	14	14
Si	2.95	2.89	2.94	2.92	3.01	2.97	3.49	3.18	3.01	3	2.76	2.75
Ti	0	0	0	0	0	0	0.01	0	0	0	0.01	0
Al	1.91	1.99	1.94	1.97	1.9	1.91	2.03	2.62	0.99	1	2.62	2.59
Cr	0	0	0	0	0	0	0.01	0	0	0	0	0
Fe^{3+}	0.11	0.11	0.11	0.11	0.11	0.11	0	0	0	0	0	0
Fe^{2+}	2.32	2.33	2.43	2.44	1.94	1.85	0.13	0.08	0	0	2.19	2.13
Mn	0.33	0.25	0.12	0.1	0.06	0.08	0	0	0	0	0.01	0.01
Mg	0.15	0.27	0.24	0.3	0.28	0.15	0.32	0.13	0	0	2.33	2.47
Ca	0.26	0.2	0.25	0.2	0.67	0.95	0	0	0.01	0.01	0	0
Na	0.02	0.02	0.01	0.03	0.03	0.02	0.08	0.17	0.98	0.97	0.01	0
K	0	0	0	0	0	0	0.89	0.81	0	0.01	0	0
X（phase）	0.05	0.05	0.08	0.1	0.07	0.03					0.48	0.46
Y（phase）	0.1	0.1	0.09	0.04	0.4	0.53						

注：(g)=Xpy =Mg／(Fe + Mn + Mg + Ca); Y(g) = Xgr=Ca／(Fe + Mn + Mg + Ca); X(chl)=Fe^{2+}/(Fe^{2+}+Mg)
g−C:石榴石核部；g−M:石榴石幔部；g−R:石榴石边部；mu−R: 石榴石边部的白云母；ab：钠长石；chl：绿泥石

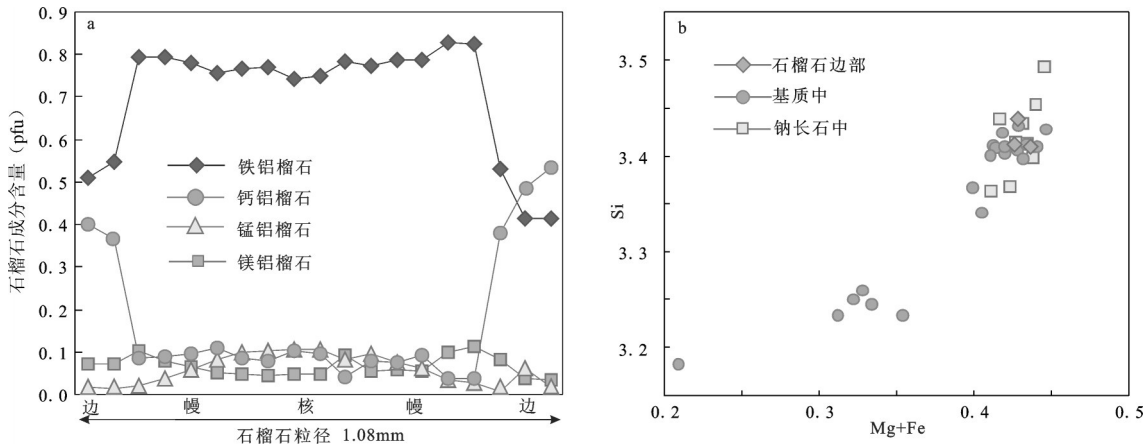

图4 a—松多含石榴石云母石英片岩的石榴石成分剖面；(b—松多含石榴石云母石英片岩中多硅白云母的(Fe+Mg)−Si成分图

Fig. 4 a−Zoning profiles of garnet grains from Sumdo garnet−bearing mica−quartz schist; b−(Fe+Mg) versus Si pfu diagram for phengite in Sumdo garnet−bearing mica−quartz schist

X_{alm} = Fe^{2+} /(Fe^{2+} + Mn + Mg + Ca), X_{py} = Mg /(Fe^{2+} + Mn + Mg + Ca), X_{gr} = Ca /(Fe^{2+} + Mn + Mg + Ca), X_{sps} = Mn /(Fe^{2+} + Mn + Mg + Ca);（X_{alm}：铁铝榴石 (almandine)；X_{prp}：镁铝榴石 (pyrope)；X_{grs}：钙铝榴石 (grossular)；X_{sps}：锰铝榴石 (spessartine)）

表2 松多含石榴石云母石英片岩(13SD24)的全岩化学成分(%)及有效全岩成分(%)

Table 2 Whole-rock and effective compositions of Sumdo garnet-bearing mica-quartz schist (13SD24)

样品 13SD24	SiO_2	Al_2O_3	CaO	Fe_2O_3	FeO	K_2O	MgO	MnO	Na_2O	TiO_2	P_2O_5	LOI	Total
XRF 分析	72.01	13.00	0.94	0.75	2.98	2.82	1.53	0.07	2.15	0.57	0.12	2.42	99.36
有效全岩成分	80.31	8.53	1.12	0.31	2.77	2.01	2.56	0.07	2.32				100

软件计算出*P*-*T*视剖面图、和*P*-M(H_2O)视剖面图,模拟并推断岩石变质演化过程的研究方法,此方法基于岩石的全岩地球化学成分,它对模拟过程有着至关重要的影响。

样品13SD24的全岩地球化学成分是在国家地质实验测试中心通过XRF技术分析所得(表2),Fe_2O_3含量采用湿化学法测定而得。从全岩成分上看,岩石具有较高的Al_2O_3与K_2O含量,显示出泥质片岩的特点[55]。

4　相平衡模拟及*P*-*T*演化

根据含石榴石云母石英片岩的矿物组合与矿物成分,本文选择在MnO-Na_2O-CaO-K_2O-FeO-MgO-Al_2O_3-SiO_2-H_2O-O(Fe_2O_3)(MnNCKFMASHO)体系中模拟其矿物组合变化特征及变质演化过程。虽然全岩成分中MnO含量较低,但是它对石榴石的稳定域有较大影响[65-70],因此将其保留。TiO_2主要赋存在副矿物金红石及榍石中,P_2O_5主要赋存在磷灰石中,这些矿物在岩石中含量均很少,并且这两个组分对相关系的影响很小,因此本文将TiO_2与P_2O_5从全岩成分中剔除。流体相设为纯水,并设水、石英和多硅白云母过剩。

本文利用*P*-*T*和*P*-M(H_2O)视剖面图来阐明松多含石榴石云母石英片岩的相关系。计算视剖面图所使用的全岩成分换算成模式体系中的mole百分比。相平衡模拟使用程序Thermocalc 3.33(2009年7月更新)[71],数据库选择tc-ds.55txt [72] (2003年11月更新)。所涉及矿物相的活度-成分关系为纤柱石[70]、石榴石[73]、绿辉石和硬玉[74]、黑云母[75]、绿泥石[76]、钠云母和多硅白云母[77],硬柱石、钠长石、石英和水为纯端元相。

含石榴石云母石英片岩(样品13SD24)在MnNCKFMASHO体系下的*P*-*T*视剖面图(图5-a、b)以四变域、五变域和六变域为主,三变域很少,不含双变域。为了准确限定岩石变质演化过程中的温压条件,本文在*P*-*T*视剖面图中计算了石榴石的镁铝榴石等值线、钙铝榴石等值线和多硅白云母的Si含量等值线(图5-a)。此外,为了详细地讨论岩石的变质作用演化过程及流体行为,本文还在*P*-*T*视剖面图中计算了相应矿物组合中饱和水含量等值线(图5-a)。

样品(13SD24)现存矿物组合(g-Chl-Ab-Bi(+Phn+q+H_2O))在图5-a中稳定的*P*-*T*范围是(2~5)×10^5 kPa,400~549℃。如果将实测石榴石的镁铝榴石(X_{prp})和钙铝榴石含量(X_{grs})投影到*P*-*T*视剖面图中(图5-a),可以发现,现存石榴石保存的生长记录主要落在(21~27)×10^5 kPa,460~520℃(核部及幔部)和(6~7.5)×10^5 kPa,520~580℃(边部)的温压范围内,并且多硅白云母的最高硅含量与最高镁铝榴石含量的交点(大约25.9×10^5 kPa/523℃)也落在石榴石幔部记录的温压范围内(图5-a)。因此,现存矿物组合并不是平衡共生的矿物组合,石榴石和多硅白云母记录了早期的变质演化过程,而绿泥石、钠长石和黑云母则代表了后期角闪岩相及绿片岩相退变叠加的结果。如图5-a所示,石榴石从核部到幔部的成分值(C→M)可限定出一条进变质的*P*-*T*轨迹,依次穿过四变域g-Jd-Law-Chl-Cr(+Phn+q+H_2O)和五变域g-Jd-Law-Cr(+Phn+q+H_2O),指示温压条件从大约21×10^5 kPa/450℃到大约26.9×10^5 kPa/520℃的升压升温过程,此时与石榴石共生的矿物为纤柱石、硬柱石、硬玉、绿泥石、多硅白云母和石英。石榴石边部成分(R1/R2)分别落在四变域g-O-Bi-Ab-Pa(+Phn+q+H_2O)和g-O-Bi-Ab-Chl(+Phn+q+H_2O)及五变域g-O-Bi-Ab(+Phn+q+H_2O)中,所限定的温压条件为(6~7.5)×10^5 kPa和520~580℃。如图4所示,石榴石镁铝榴石含量从幔部到边部突然降低,锰铝榴石含量从幔部到边部突然升高,表明石榴石边部成分受到了后期退变质改造,不代表峰期变质条件。

如图5-a所示,岩石变质过程中由石榴石及多

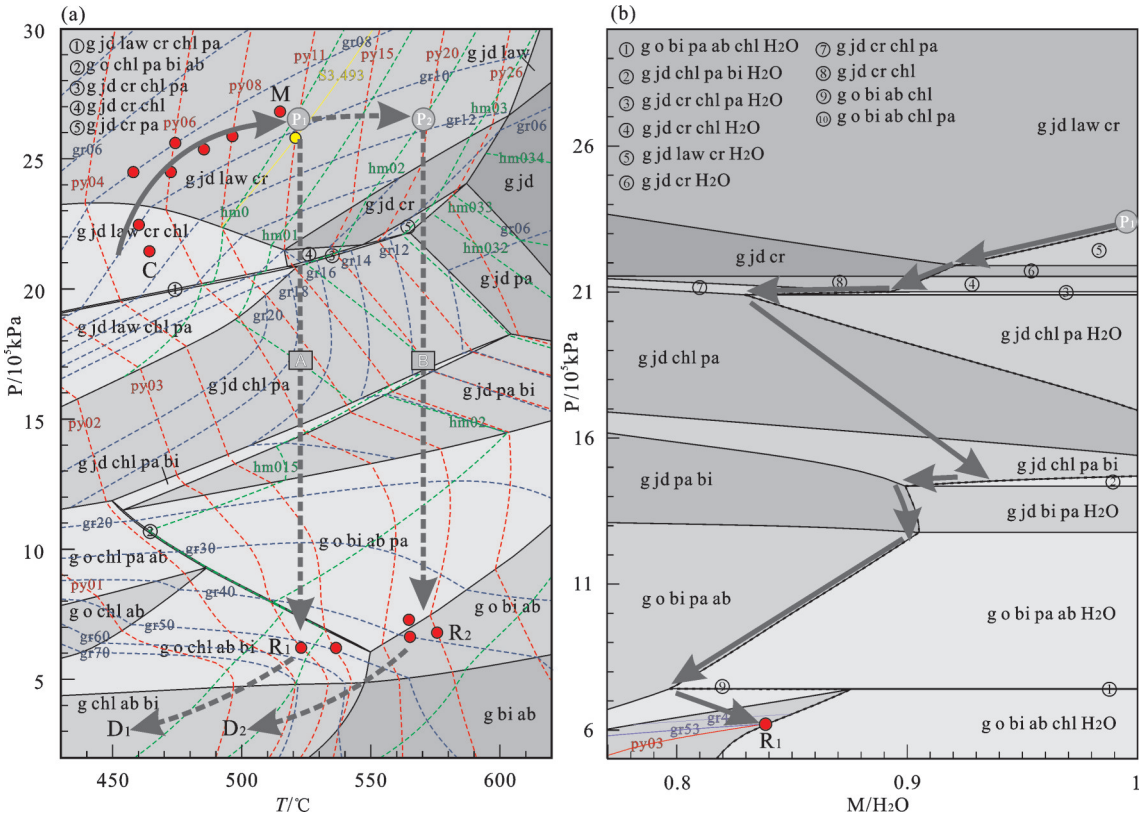

图5 样品13SD24在MnNCKFMASHO(+Phn+q/Coe+H_2O)体系下视剖面图

a—*P*−*T*视剖面图,计算时使用的全岩成分见表2;其中,三变域标示为无色,四变域、五变域、六变域、七变域逐渐从浅灰色变为深灰色;图中包含主要稳定域矿物组合、相应的石榴石中镁铝榴石和钙铝榴石成分含量等值线、多硅白云母Si−含量等值线和饱和水含量等值线,红色圆圈代表石榴石环带成分点,黄色圈圈代表多硅白云母硅含量投点,与图4 和表1对应。b—石英、云母过量时,在温度523℃时计算出的P−M(H_2O)图 ,红色圆圈代表石榴石边部成分点

Fig. 5 The pseudosection in the MnNCKFMASHO system (+phn+q/coe+H_2O) for sample 13SD24

a−The bulk composition used in this pseudosection from Table 2; The trivariant fields are unshaded, quadrivariant fields are lightly shaded, and the quinivariant fields, hexa− and heptavariant fields are increasingly shaded; The pseudosections contain the main mineral assemblages, contoured with isopleths of grossular and pyrope values in garnet for the corresponding mineral assemblages, isopleths of Si content in phengite and saturated H_2O content contours. Projection of the garnet and phengite compositions are shown as red and yellow circles with the label C, M, R1, R2 corresponding to those in Fig. 4 and Table 1.b−P−M(H_2O) pseudosection at 523℃ with excessive quartz, phengitic muscovite, but without H_2O for sample 13SD24, garnet rim compositions are shown as red circles

硅白云母的成分所记录的温度最大值与压力最大值不能同时达到,结合岩石中矿物饱和水等值线的变化,认为岩石在M点以后可能经历A、B两种不同的*P*−*T*演化轨迹。变质演化过程若按轨迹A进行,则岩石在到达石榴石幔部成分点(M)所记录的温压条件后,随即等温降压到石榴石边部成分点记录的位置,变质峰期P1为石榴石幔部成分(M)所记录的矿物组合g−Cr−Jd−Law(+Phn/Coe+q+H_2O)与其对应的温压条件为大约26.5×10^5 kPa/523℃,这与大别山和西南天山超高压变泥质−长英质片麻岩所纪录的抬升轨迹一致[20,25]。晚期阶段降温降压至现阶段所保存的矿物组合稳定域g−Chl−Bi−Ab(+Phn+q+H_2O)中,此期间经历四个阶段的脱水作用过程,主要变质反应及矿物组合演化在相应阶段依次发生。峰期之后第一次脱水作用,*P*−*T*轨迹依次穿过g−Cr−Jd(+Phn+q+H_2O)、五变域g−Chl−Jd−Cr(+Phn+q+H_2O)、四变域g−Jd−Cr−Chl−Pa(+Phn+q+H_2O),并切割矿物饱和水含量降低的等值线(图5−a),有利于矿物组合演化[78−79],先后发生脱水反应g+Law=Cr+Chl+Jd+H_2O、g+Cr=Chl+Jd+Pa+H_2O,导致石榴石大量被消耗,成分受到改造,硬玉、绿泥石及钠云母生长,硬柱石和纤柱石分别于22×10^5 kPa和

21×10^5 kPa左右的压力处消失(图5-b)。此过程中,矿物脱去大量的水,若没有外来流体的加入体系将处于流体缺失状态,岩石进入流体缺失的变质演化阶段(图5-b)。随后岩石进入五变域g-Jd-Chl-Pa(+Phn+q+H_2O),*P*-*T*轨迹沿着矿物中饱和水含量升高的方向切割饱和水含量等值线(图5-a、b),不利于矿物组合的演化,不发生变质反应,峰期矿物组合在该阶段易于保存[79]。当*P*≈14.9×10^5 kPa时,岩石进入四变域g-Jd-Chl-Pa-Bi(+Phn+q+H_2O),此后将经历第二次脱水作用,发生脱水反应g+Jd+Chl=Bi+Pa+H_2O,使得早期绿泥石消失,黑云母在此阶段生长,而后*P*-*T*轨迹进入五变域g-Jd-Bi-Pa(+Phn+q+H_2O)中,此稳定域矿物中饱和水含量依然略有增长,不发生变质反应,未保存有石榴石生长或者被消耗的记录。当*P*≈12.9×10^5 kPa时,钠长石出现,硬玉转变为绿辉石,*P*-*T*轨迹依次进入四变域g-O-Bi-Pa-Ab(+Phn+q+H_2O)、三变域g-O-Bi-Pa-Ab-Chl(+Phn+q+H_2O)和四变域g-O-Bi-Chl-Ab(+Phn+q+H_2O)中,岩石在四变域g-O-Bi-Pa-Ab(+Phn+q+H_2O)和g-O-Bi-Chl-Ab(+Phn+q+H_2O)发生第三次及第四次脱水反应。四次脱水反应使得石榴石边部成分发生改造,并在五变域g-O-Bi-Chl-Ab(+Phn+q+H_2O)中被记录下来。岩石在石榴石边部记录的温压条件后开始降温降压至五变域g-Chl-Ab-Bi(+Phn+q+H_2O),即薄片中所观察到的矿物组合。

此外,由于石榴石边部成分点所记录的最大温度要高于峰期P1所对应的温度条件,因此,在岩石到达石榴石幔部成分(M)记录的温压条件之后,推测*P*-*T*轨迹将切割水含量降低的矿物饱和水等值线沿着近等压升温的路径演化至峰期P2(约26.5×10^5 kPa/580℃),即轨迹B。如图5-a(B)所示,此峰期温度与石榴石边部成分点所记录的最大温度一致。峰期之后,岩石先经历早期近等温降压过程至石榴石边部成分点所记录的温压条件,而后降温降压至现阶段保存的矿物组合稳定域g-Chl-Ab-Bi(+Phn+q+H_2O)。岩石在变质演化过程中的流体行为与轨迹A基本一致,这种情况可以解释为,早期的脱水反应及峰期后岩石所经历的严重退变作用使得峰期变质条件受到改造而未能保存下来。

综合以上分析,早期绿泥石在进变质阶段消失,岩石中可观察到的绿泥石可能为晚期退变质作用生成,再结合岩相学特征,石榴石中的云母包体形成于早期进变质阶段,切穿片理的云母和石榴石"假象"中的云母可能是晚期重结晶或者变质结晶而得。据此可以推论,样品中的的绿泥石、石榴石、钠长石、白云母、黑云母及石英为岩石在进变质、峰期或者退变质的不同阶段所保存下来的产物。

5 讨　论

5.1 松多含石榴石石英云母片岩的变质演化

根据松多含石榴石云母石英片岩的岩相学特征、矿物化学特征和相平衡模拟结果,本文将该类岩石的变质演化过程划分为三个阶段:进变质阶段、峰期变质阶段和退变质阶段。

5.1.1 进变质阶段

进变质阶段主要由石榴石核部到幔部的成分确定,表现为从大约21×10^5 kPa/450℃升温升压至大约26.5×10^5 kPa/523℃,若按图5-a轨迹A演化,幔部成分点所记录的温压条件即为变质峰期,若按图5-a轨迹B演化,岩石到达幔部成分点所记录的温压条件之后,将继续升温升压至变质峰期P2(约26.5×10^5 kPa/580℃)。该阶段*P*-*T*轨迹不断切割饱和水含量降低的等值线,有利于矿物组合的演化,并发生脱水反应Chl+Law+Cr=g+Jd+Phn+H_2O,导致早期生成的绿泥石消失,石榴石、硬玉和多硅白云母生长,石榴石在该阶段记录进变质环带。从图6的*P*-*T*轨迹可以看出,含石榴石云母石英片岩经历了从蓝片岩相到榴辉岩相的变质演化过程,是典型的冷俯冲过程。与之相比,包裹在片岩中的蓝闪石榴辉岩[38]经历了快速升压缓慢升温的进变质演化过程,虽然二者具有不同的进变质*P*-*T*轨迹,但都代表了升温升压的冷俯冲过程。

5.1.2 峰期变质阶段

相平衡模拟的峰期变质温压条件为约26.5×10^5 kPa/523℃或者约26.5×10^5 kPa/580℃,对应的峰期矿物组合均为g-Jd-Law-Cr(+Phn+q/Coe+H_2O)。从图6可以看出,岩石在峰期经历了硬柱石-榴辉岩相或者绿帘石-榴辉岩相的变质作用。石榴石的边部成分并未记录变质峰期,石榴石成分环带特征和相平衡模拟表明其受到了后期的退变质改造。岩石中普遍存在的钠长石变斑晶包裹白云母

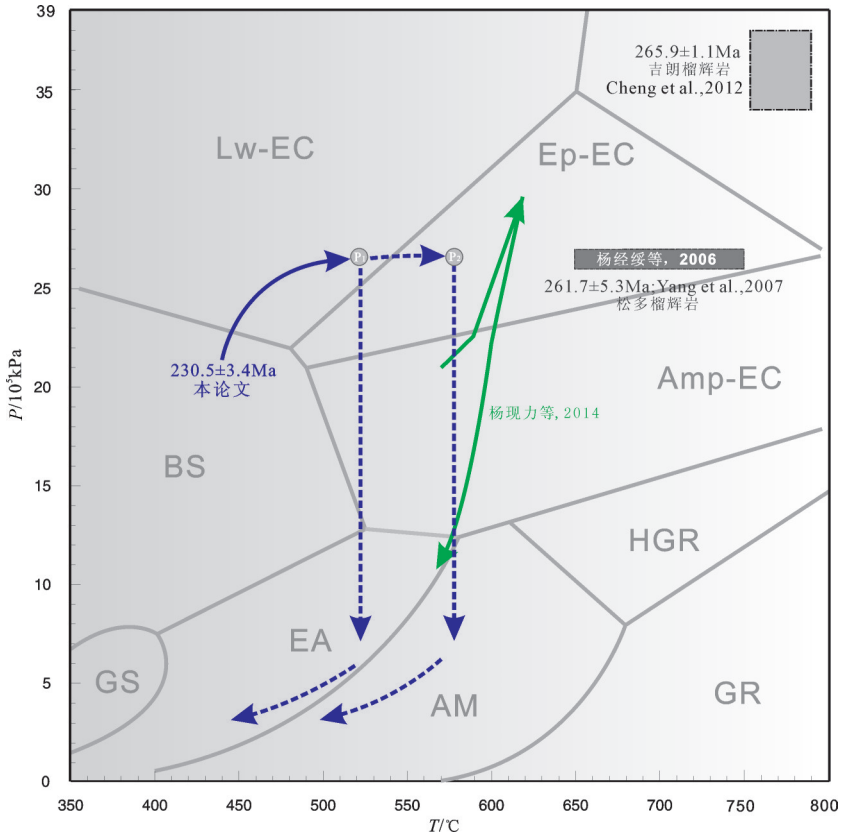

图6 研究区峰期温压条件及年龄对比图

相图中灰色实线所划分的岩相根据参考文献[54]修改；本研究所得PT轨迹以深灰色标注，黑色PT轨迹为杨现力等2014[38]对松多榴辉岩进行相平衡模拟所得；其余用温压计限定的松多榴辉岩或者其围岩的峰期温压条件均以不同颜色标定于图中。Lw-EC—硬柱石榴辉岩相；Ep-EC—绿帘石榴辉岩相；Amp-EC—角闪石榴辉岩相；BS—蓝片岩相；GS—绿片岩相；EA—绿帘角闪岩相；AM—角闪岩相；GR—麻粒岩相；HGR—高压麻粒岩相

Fig.6 The comparison of peak metamorphic conditions and metamorphic ages in the study area

The gray lines show the boundaries of different facies proposed by Zhang et al.2014[38]; The dark gray dashed lines and solid lines show the P-T path in this paper; The black solid arrows show the P-T path modeled by Yang et al. 2014; other peak P-T conditions of eclogite or relevant country rocks are shown by different colors. Lw-EC-Lawsonite-eclogite facies; Ep-EC-Epidote--eclogite facies; Amp-EC-Amphibolite-eclogite facies; BS-Blueschist facies; GS-Greenschist facies; EA-Epidote-amphibolite facies; AM-Amphibolite facies; GR-Granulite facies; HRG-HP granulite facies

和石英等矿物，推测其可能为峰期硬玉的退变质产物[25,38]。相平衡模拟同样表明，岩石在进变质阶段、峰期变质阶段与早期近等温降压抬升阶段均有硬柱石、纤柱石存在，但在岩石中并未发现硬柱石、纤柱石或二者的假象。前人研究发现，硬柱石的形成需要大量的水，快速折返或者足够冷的抬升条件才可以使其保存下来，在自然状态的岩石中，很少发现有硬柱石存在[78, 80]，拉萨地块近等温降压的抬升过程会使硬柱石脱水转变为绿帘石[58]。纤柱石由于其稳定域较窄，在折返过程中同样需要较快的侵出速率及足够冷的抬升条件才能保存下来[70]。此外，全岩成分对纤柱石的保存也会产生影响[81]。

杨经绥等(2006)[28]利用g-O-Phn压力计和g-O、g-Phn温度计算出松多榴辉岩的峰期温压条件为(26~27)×10⁵ kPa，650~750℃；杨现力等(2014)[38]通过相平衡模拟方法限定出松多蓝闪石榴辉岩的峰期温压条件为大约30×10⁵ kPa，大约610℃；本文得出的压力条件能达到二者所限定的高压范围，本文所限定的温度也与杨现力等(2014)[38]所得到的中温条件一致(图6)。Cheng (2012)[34]采用相平衡模拟计算出邻近地区吉朗榴辉岩的峰期矿物组合g-O-phn-Coe，峰期温压条件为(34~38)×10⁵ kPa，753~790℃，高于本文样品的峰期温压条件，魏春景等(2013)[45]指出在榴辉岩峰期矿物组合g-O-Phn-

Coe中石榴石和多硅白云母的成分易于受全岩成分的影响,难以利用它们的成分等值线有效地限定岩石的温压条件,因此Cheng (2012)[34]所模拟的峰期温压条件可能是不准确的。

5.1.3 退变质阶段

岩石在变质峰期之后,先经历早期的近等温降压阶段,发生四次脱水作用,第一次脱水发生在抬升早期,进变质阶段生长的纤柱石、硬柱石随脱水反应消失,石榴石遭受改造成分发生变化,此后岩石进入流体缺失的状态。二三次四次脱水作用在岩石处于贫流体的状态下发生,第二次脱水作用反应导致早期绿泥石消失,脱去的水使得黑云母生长。三四次脱水后,钠质单斜辉石硬玉由于钠长石的出现脱去钠质成分转变为绿辉石,晚期退变绿泥石出现,部分取代石榴石或生长于石榴石的裂隙中,少量白云母转变为黑云母,石榴石边部成分遭受四次脱水作用后被改造。当$P-T$轨迹演化到与峰期矿物组合水含量相同的温压条件处(6×10^5 kPa,523℃),受到改造的石榴石边部成分被记录下来。晚期岩石经历降温降压的退变质过程至现阶段岩石的矿物组合稳定域g−Ab−Bi−Chl(+Phn+q+H_2O)。从图6中可以看出,含石榴石云母石英片岩在退变质早期阶段经历了角闪岩相至绿帘角闪岩相的变质作用,晚期阶段遭受了绿片岩相叠加。

5.2 松多含石榴石石英云母片岩的构造意义

本论文利用MnO−Na_2O−CaO−K_2O−FeO−MgO−Al_2O_3−SiO_2−H_2O−O(Fe_2O_3)(MnNCKFMASHO)体系通过Thermocalc对含石榴石云母石英片岩进行相平衡模拟,限定了岩石的峰期变质温压以及$P-T$演化轨迹,将其与前人所做研究进行对比(图9)可以发现,该片岩与榴辉岩在理论上峰期变质温度可以达到一致,进变质轨迹与杨现力等(2014) 所提出的进变质轨迹略有出入[38],但整体都反映了一个升温升压的冷俯冲过程,退变质阶段它与榴辉岩经历了基本相同的早期近等温降压及晚期降温降压的退变质过程。此外,据野外露头观察,含石榴石石英云母片岩与榴辉岩接触伴生。这些证据可以为证明松多榴辉岩围岩含石榴石石英云母片岩曾经历过高压变质,与榴辉岩有着相同或者相似俯冲折返过程提供重要证据。

本研究得出的松多榴辉岩围岩−含石榴石云母石英片岩的变质温压条件支持了前人的研究,认为松多榴辉岩带可能代表了一条新的高压变质带,这表明拉萨地块中可能存在板块深俯冲作用以及板块缝合带[28],大约266 Ma的榴辉岩相变质时代,说明可能安第斯型造山时期古特提斯洋盆俯冲导致了高压变质的发生[28,30,34,36,40,50,52,54,58],榴辉岩带中伴随着超镁铁岩、大洋和洋岛玄武岩等蛇绿岩带的岩石组合,同样也为缝合带的存在提供了证据[38,62]。此外,松多榴辉岩围岩经历过高压变质的温压条件同时也为晚古生代—早中生代中压变质带的划分提供了新的依据。松多榴辉岩与其围岩含石榴石云母石英片岩在峰期后的减压阶段均经历等温降压的退变质过程[38],表明它们侵出速度很快,自身浮力或者与之伴生的蛇纹岩化地幔橄榄岩所产生的牵引力−浮力等可作为岩石上升至低地壳的侵位机制[25,82−84]。等温降压的过程中,含石榴石云母石英片岩经历了角闪−榴辉岩相至角闪岩相的变质作用,后期复杂的碰撞造山作用导致岩石从低地壳快速上升至地表,并伴随有绿帘角闪岩相−绿片岩相变质的叠加。

6 结　论

(1)岩石中石榴石具有从核到幔Xprp升高,Xsps降低的生长环带,其边部成分受到后期变质的改造,显示出Xprp降低,Xgrs升高的特点。利用NCKMnFMASHTO体系中的$P-T$视剖面图,结合石榴石成分值和饱和水等值线确定了松多含石榴石石英云母片岩可能的$P-T$演化轨迹,并限定出峰期变质条件约26.5×10^5 kPa,523/580°C,对应的峰期矿物组合为g−Jd−Law−Cr(+Phn+q+H_2O)。

(2)石榴石核部到幔部成分环带记录了主要的进变质$P-T$轨迹,结合饱和水等值线的变化,推断出岩石在进变质阶段经历了升温升压的冷俯冲过程,并经历蓝片岩−榴辉岩相变质。峰期后含石榴石云母石英片岩将经历早期近等温减压的快速折返抬升的过程,经历绿帘角闪岩−角闪岩相变质,四次脱水作用使得石榴石边部成分被改造,后期通过降温降压的退变质过程继续折返至地表,并遭受绿片岩相变质的叠加。

(3)对比松多含石榴石石英云母片岩与榴辉岩的峰期变质条件、$P-T$轨迹以及变质演化过程,并

结合二者在野外相互伴生的地质关系,证明了松多榴辉岩与其围岩含石榴石石英云母片岩一起经历高压变质,有着相同或者相似的俯冲折返过程。

致谢:感谢中国地质科学院陈松永副研究员在野外工作中的帮助及北京大学地球与空间科学学院李小黎博士在电子探针实验过程中的帮助。北京大学地球与空间科学学院余黄露对相图模拟给予了很大的帮助,在此表示诚挚的谢意。

参考文献(References):

[1] Coleman R G, Wang XiaoMing. Ultrahigh Pressure Metamorphism[C]//Cambridge Topics in Petrology. Cambridge University Press, 1995, UK. p. 528.

[2] Chopin C. Coesite and pure pyrope in high−grade blueschists of the Western Alps; a first record and some consequences [J]. Contributions to Mineralogy and Petrology,1984, 86:107−118.

[3] Chopin C. Ultrahigh−pressure metamorphism: tracing continental crust into the mantle [J]. Earth and Planetary Science Letters, 2003, 212: 1−14.

[4] Carswell D A.Eclogite Facies Rocks [M].Blackie, New York, 1990: 396.

[5] Ernst W G. Subduction, ultrahigh−pressure metamorphism and regurgitation of buoyant crustal slices: Implications for arcs and continental growth [J]. Physics of the Earth and Planetary Interiors, 2001,127:253−275.

[6] Ernst W G. Preservation/exhumation of ultrahigh−pressure subduction complexes [J]. Lithos, 2006,92:321−335.

[7] Maruyama S, Liou J G , Tarabayashi M. Blueschists and eclogites of the world and their exhumation[J]. International Geology Review, 1996,38:485−594.

[8] Smith D C.A review of the peculiar mineralogy of the Norwegian coesite−eclogite province, with crystal−chemical, petrological, geochemical and geodynamical notes and an extensive bibliography[C]//Smith D C(ed.). Eclogites and Eclogite Facies Rrocks. Amsterdam:Elsevier, 1988: 1−206.

[9] Song Shuguang, Zhang Lifei, Niu Yaoling, et al. Evolution from oceanic subduction to continental collision: A case study of the northern Tibetan Plateau inferred from geochemical and geochronological date [J]. Journal of Petrology, 2006, 47: 435−455.

[10] Zhang Lifei, Lü Zeng, Zhang Guibin, et al. The geological characteristics of oceanic−type UHP metamorphic belts and their tectonic implications: Case studies from Southwest Tianshan and North Qaidam in NW China [J]. Chinese Science Bulletin,2008, 53: 3120−3130.

[11] Ko Z W, Enami M, Aoya M. Chloritoid and barroisite−bearing pelitic schists from the eclogite unit in the Besshi district, Sanbagawa metamorphic belt [J]. Lithos, 2005,81:79−100.

[12] Okay A I. An exotic eclogite blueschist slice in a Barrovian−style metamorphic terrain, Alanya nappes, Southern Turkey [J]. Journal of Petrology, 1989, 30: 107−132.

[13] Wallis S, Aoya M. A reevaluation of eclogite facies metamorphism in SW Japan: Proposal for an eclogite nappe [J]. Journal of Metamorphic Geology, 2000, 18: 653−664.

[14] Liou J G, Zhang Ruyuan. Ultrahigh−pressure metamorphic rocks: Encyclopedia of Physical sciences and technology [J]. Thirded., Tarzana, CA, Academia Press, 2002: 227−244.

[15] Zhang Jianxin, Meng Fancong, Yang Jingsui. Eclogitic metapelites in the western segment of the north Qaidam Mountains: Evidence on "in situ" relationship between eclogite and its country rocks [J]. Science in China (Series D), 2004,12: 1102−1112.

[16] Zheng Yongfei, Fu Bin, Gong Bing, et al. Stable isotope geochemistry of ultrahigh−pressure metamorphic rocks from the Dabie—Sulu orogen in China: Implications for geodynamics and fluid regime [J]. Earth Science Review, 2003, 62: 105−161.

[17] 张贵宾,张立飞,宋述光. 柴北缘超高压变质带:从大洋到大陆的深俯冲过程[J]. 高校地质学报, 2012,18(1):28−40.
Zhang Guibin, Zhang Lifei, Song Shuguang. An overview of the tectonic evolution of north Qaidam UHPM belt: from oceanic subduction to continental collision [J]. Geological Journal of China Universities, 2012,18(1): 28−40(in Chinese with English abstract).

[18] Proyer A. The preservation of high−pressure rocks during exhumation: metagranites and metapelites [J]. Lithos, 2003, 70: 183−194.

[19] P S ˇ TI´PSKA´, P PITRA, R POWELL. Separate or shared metamorphic histories of eclogites andsurrounding rocks? An example from the Bohemian Massif [J].Journal of Metamorphic Geology, 2006, 24: 219−240.

[20] Carswell D A, Zhang Ruyuan. Petrographic characteristics and metamorphic evolution of ultrahigh−pressure eclogites in the plate−collision belts[C]//ErnstW G, LiouJ G(eds.). Ultra−high Pressure Metamorphism and Geodynamics in Collision−type Orogenic Belts. Columbia, MD: Bellwether, 2000: 39−56.

[21] Krogh E J. Metamorphic evolution of Norwegian country−rock eclogites, as deduced from mineral inclusions and compositional zoning in garnets[J]. Lithos, 1982, 15: 305−321. Oslo. ISSN 0024−4937.

[22] Menold C A, Manning C E, Yin A, et al. Metamorphic evolution, mineral chemistry and thermobarometry of orthogneiss hosting ultrahigh−pressure eclogites in the north Qaidam metamorphic belt, western China [J]. Journal of Asian Earth Sciences, 2009,35: 273−284.

[23] Marian Jana´k, David Cornrll, Nikolaus Froitzheim, et al. Eclogite−hosting metapelites from the Pohorje Mountains (Eastern Alps): *P*−*T* evolution, zircon geochronology and tectonic

implications [J]. Journal of Mineral, 2009,21:1191−1212.

[24] R T Orozbaev, A Takasu, A B Bakirov, et al. Metamorphic history of eclogites and country rock gneisses in the Aktyuz area, Northern Tien− Shan, Kyrgyzstan: a record from initiation of subduction through to oceanic closure by continent− continent collision [J]. Journal of Metamorphic Geology,2010,28:317−339.

[25] Wei Chunjing, Wang Wei, Clarke G L, et al. Metamorphism of high/ultrahigh− pressure politic− felsic schist in the South Tianshan orogen, NW China: phase equilibria and *P*−*T* path [J]. Journal of Petrology 2009,50:1973−1991.

[26] 陈松永, 杨经绥, 徐向珍, 等. 西藏拉萨地块松多榴辉岩的锆石Lu/Hf同位素研究及LA−ICP−MS U−Pb定年[J].岩石学报, 2008, 24: 1528−1538.
Chen Songyong, Yang Jingsui, Xu Xiangzhen, et al. Zircon LA−ICP− MS U− Pb and garnet Lu− Hf geochronology of Sumdo eclogites from the Lhasa Block, Tibet[J].Acta Petrologica Sinica, 2008, 24: 1528−1538(in Chinese with English abstract).

[27] 徐向珍, 杨经绥, 李天福, 等. 青藏高原拉萨地块松多榴辉岩的锆石SHRIMP U−Pb年龄及锆石中的包裹体[J]. 地质通报, 2007, 26: 1340−1355.
Xu Xiangzhen, Yang Jingsui, Li Tianfu, et al. SHRIMP U− Pb ages and inclusions of zircons from the Sumdo eclogite in the Lhasa block, Tibet, China [J]. Geological Bulletin of China, 2007, 26:1340−1355(in Chinese with English abstract).

[28] 杨经绥, 许志琴, 耿全如, 等. 中国境内可能存在一条新的高压/超高压(？)变质带−−青藏高原拉萨地块中发现榴辉岩带[J].地质学报, 2006, 80: 1787− 1792.
Yang Jingsui, Xu Zhiqin, Geng Quanru, et al. Apossible new HP/UPH metamorphic belt in China: Discorvery of eclogites in the Lhasa terrane, Tibet [J]. Acta Geologica Sinica , 2006,80:1788−1792(in Chinese with English abstract).

[29] 杨经绥，许志琴，李天福，等. 青藏高原拉萨地块中的大洋俯冲型榴辉岩：古特提斯洋盆的残留[J]？地质通报,2007,26:1277−1287.
Yang Jingsui, Xu Zhiqin, Li Tianfu, et al. Oceanic subduction−type eclogite in the Lhasa block, Tibet, China: Remains of the Paleo−Tethys ocean basin [J]? Geological Bulletin of China, 2007, 26:1277−1287(in Chinese with English abstract).

[30] Yang Jingsui, Xu Zhiqin, Li Zhaoli, et al. Discovery of an eclogite belt in the Lhasa block, Tibet: A new border for Paleo−Tethys? [J]. Journal of Asian Earth Sciences, 2009,34: 76−89.

[31] Pan G, Ding J, Yao D, et al. Geological Map of the Qinghai−Xizang (Tibet) Plateau and Adjacent Areas[R].Chengdu Cartographic Publishing House, Chengdu, 2004.

[32] Pan Guitang, Mo Xuanxue, Hou Zengqian, et al. Spatial−temporal framework of the Gangdese orogenic belt and its evolution [J].Acta Petrologica Sinica, 2006,22:521−533.

[33] Zhu Dicheng, Zhao Zhidan, Niu Yaoling, et al. The Lhasa Terrane: record of a microcontinent and its histories of drift and growth [J]. Earth and Planetary Science Letters, 2011, 301: 241−255.

[34] Cheng Hao, Zhang Chao, Vervoot J D, et al. Zircon U− Pb and garnet Lu− Hf geochronology of eclogites from the Lhasa Block, Tibet [J]. Lithos, 2012, 155:341−359.

[35] 陈松永, 杨经绥, 罗立强, 等. 西藏拉萨地块MORB型榴辉岩的岩石地球化学特征[J].地质通报,2007,26:1327−1339.
Chen Songyong, Yang Jingsui, Luo Liqiang, et al. MORB− type eclogites in the Lhasa block, Tibet, China: Petrochemical evidence [J]. Geological Bulletin of China, 2007, 26: 1327−1339. (in Chinese with English abstract).

[36] Li Zhaoli, Yang Jingsui, Xu Zhiqin, et al. Geochemistry and Sm−Nd and Rb− Sr isotopic composition of eclogite in the Lhasa terrane, Tibet, and its geological significance [J]. Lithos, 2009, 109: 240−247.

[37] 张丁丁，张立飞，赵志丹. 西藏松多榴辉岩变质作用研究[J].地学前缘, 2011,18(2):116−126.
Zhang Dingding, Zhang Lifei, Zhao Zhidan. A study of metamorphism of Sumdo eclogite in Tibet, China [J].Earth Science Frontires, 2011,18(2):116− 126(in Chinese with English abstract).

[38] 杨现力，张立飞，赵志丹，等. 青藏高原拉萨地块松多蓝闪石榴辉岩的变质演化:相平衡及变质作用*P*−*T*轨迹[J]. 岩石学报, 2014, 30(5):1505−1509.
Yang Xianli, Zhang Lifei, Zhao Zhidan, et al. Metamorphic evolution of glaucophane eclogites from Sumdo, Lhasa block of Tibetan Plateau: Phase equilibria and metamorphic *P*−*T* path [J]. Acta Petrologica Sinica, 2014, 30(5) : 1505− 1519. (in Chinese with English abstract).

[39] 杨德明, 和钟铧, 黄映聪, 等. 西藏墨竹工卡县门巴地区松多岩群变质作用特征及时代讨论[J].吉林大学学报,2005,35:430−435.
Yang Deming, He Zhonghua, Huang Yingcong, et al. Dicussion of metamorphism and era of Sumdo group in Mamba area from maizhokunggar,Tibet [J]. Journal of Jilin University , 2005,35: 430−435(in Chinese with English abstract).

[40] Li Huaqi, Xu Zhiqin, Yang Jingsui, et al. Records of Indosinian orogenesis in Lhasa Terrane, Tibet [J]. Journal of Earth Science, 2009, 20: 348−363.

[41] Le Goff E, Bellevre M. Geothermobarometry in albite− garnet orthogneisses: a case study from the Gran Paradiso nappe (Western Alps) [J]. Lithos, 1990, 25: 261−280.

[42] 魏春景，苏香丽，娄玉行，等. 榴辉岩中传统地质温压计新解：来自*P*−*T*视剖面图的证据[J].岩石学报,2009, 25:2078−2088.
Wei Chunjing, Su Xiangli, Lou Yuxing, et al. A new interpretation of the conventional thermobarometry in eclogite: Evidence from the calculated *P*− *T* pseudosections [J]. Acta Petrologica Sinica , 2009, 25: 2078−2088 (in Chinese with English abstract).

[43] Wei Chunjing, Li Yanjuan, Yu Yang, et al. Phase equilibria and

metamorphic evolution of glaucophane− bearing UHP eclogites from the Western Dabieshan Terrane, Central China [J]. Journal of Metamorphic Geology, 2010, 28: 647−666.

[44] 魏春景.变质作用p−T−t轨迹的研究方法与进展[J]. 地学前缘, 2011,18:0001−0016.
Wei Chunjing. Approaches and advancement of the study of metamorphic P−T−t paths [J]. Earth ScienceFrontiers, 2011b,18: 0001−0016. (in Chinese with English abstract).

[45] 魏春景, 田作林, 张立飞. 高压−超高压榴辉岩的峰期矿物组合与P−T条件模拟[J]. 科学通报,2013,58:2159−2164.
Wei Chunjing, Tian Zuolin, Zhang Lifei. Modelling of peak mineral assemblages and *P*− *T* conditions for high− pressure and ultrahigh− pressure eclogites [J]. Chinese Science Bulletin,2013, 58: 2159−2164 (in Chinese).

[46] 魏春景.21世纪最初十年变质岩石学研究进展[J]. 矿物岩石地球化学通报, 2012, 31: 415−427.
Wei Chunjing. Advance of metamorphic petrology during the first decade of the 21st century [J]. Bulletin of Mineralogy Petrology and Geochemistry, 2012, 31: 415− 427 (in Chinese with English abstract).

[47] Yin A, Harrison T M. Geologic evolution of the Himalayan Tibetan Orogen [J]. Annual Review of Earth and Planetary Sciences , 2000, 28: 211−280.

[48] Zhu Dicheng, Pan Guitang, Mo Xuanxue, et al. Late Jurassic− Early Cretaceous geodynamic setting in middle− northern Gangdese: New insights from volcanic rocks [J]. Acta Petrologica Sinica, 2006, 22: 534−546.

[49] Zhu Dicheng, Mo Xuanxue, Niu Yaoling, et al. Zircon U− Pb dating and in− situ Hf isotopic analysis of Permian peraluminous granite in the Lhasa terrane, southern Tibet: implications for Permian collisional orogeny and paleogeography[J]. Tectonophysics, 2009, 469: 48−60.

[50] Zhu Dicheng, Zhao Zhidan, Pan Guitang, et al. Early Cretaceous subduction− related adakite− like rocks of the Gangdese Belt, southern Tibet: Products of slab melting and subsequent meltperidotite interaction [J]? Journal of Asian Earth Sciences, 2009, 34: 298−309.

[51] Zhu Dichen, Mo Xuanxue, Wang Liqua, et al. Petrogenesis of highly fractionated I− type granites in the Zayu area of eastern Gangdese, Tibet: constraints from zircon U− Pb geochronology, geochemistry and Sr− Nd− Hf isotopes [J]. Science in China (Series D), 2009,52: 1223−1239.

[52] Zhu Dicheng, Mo Xuaxue, Zhao Zhidan, et al. Presence of Permian extension− and arc− type magmatism in southern Tibet: paleogeographic implications [J]. GSA Bulletin , 2010,122: 979−993.

[53] Zhu Dicheng, Zhao Zhidan, Niu Yaoling, et al. The origin and pre− Cenozoic evolution of the Tibetan Plateau [J]. Gondwana Research, 2012, http://dx.doi.org/ 10.1016/j.gr.2012.02. 002.

[54] Zhang Zeming, Dong Xin, M Santosh, et al. Metamorphism and tectonic evolution of the Lhasa terrane, Central Tibet [J]. Gondwana Research, 2014, 25: 170−189.

[55] 胡道功,吴珍汉,江万,等. 西藏念青唐古拉岩群SHRIMP锆石U−Pb年龄和Nd同位素研究[J].中国科学(D辑), 2005, 35(1): 29−37.
Hu Daogong, Wu Zhenhan, Jiang Wan et al. SHRIMP U−Pb ages of zircons from dioritic gneiss in the Nyainqêntanglha Mountains, Tibet [J].Sinence in China (Series D), 2005, 35(1):29− 37 (in Chinese).

[56] 张泽明,董昕,耿官升,等.青藏高原拉萨地体北部的前寒武纪变质作用及构造意义[J].地质学报,2010,84 (4): 449−456.
Zhang Zeming, Dong Xin, Geng Guansheng, et al. Precambrian metamorphism of the Northern Lhasa Terrane Tibet and its tectonic implications [J]. Acta Geologica Sinica, 2010, 29: 1949− 1961 (in Chinese with English abstract).

[57] Zhang Zeming, Dong Xin, Liu Feng, et al. The making of Gondwana: Discovery of 650Ma HP granulites from the North Lhasa, Tibet [J]. Precambrian Research, 2012, 212−213: 107−116.

[58] Dong Xin, Zhang Zeming, Liu Feng, et al. Zircon U− Pb geochronology of the Nyainqêntanglha Group from the Lhasa terrane: new constraints on the Triassic orogeny of the south Tibet [J]. Journal of Asian Earth Sciences, 2011,42: 723−739.

[59] 西藏自治区地质矿产局.中华人民共和国区域地质调查报告,1∶200000 下巴湍(沃卡) 幅[R].北京: 地质出版社,1994.
Administration Bureau of Geology in Tibet. 1994. Report of regional geological survey in China 1∶200000 Chin Tang[R]. Beijing: Geological Publishing House(in Chinese with English abstract).

[60] 中国地质调查局成都地质矿产研究所. 青藏高原地质图1:1500000[R]. 成都:成都测绘出版社, 2004.
Chengdu institute of Geology and Mineral resources. Geological map of Tibetan Plateau, China1:1500000[R]. Chengdu: Chengdu Geomatics Press. 2004. (in Chinese).

[61] Chen Songyong, Yang Jingsui, Li Yuan, et al. Ultramafic Blocks in Sumdo Region, Lhasa Block, Eastern Tibet Plateau: An Ophiolite Unit [J]. Journal of Earth Science, 2009,20:332−347.

[62] 陈松永. 西藏拉萨地块中古特提斯缝合带的厘定[D]. 北京:中国地质科学院, 2010: 1−199.
Chen Songyong. The Development of Sumdo Suture in the Lhasa Block, Tibet[D]. Ph D Thesis, Beijing: ChineseAcademy of Geological Science, 2010: 1− 199 (in Chinese with English abstract).

[63] Li Huaqi, Cai Zhihui, Chen Songyong, et al. The Indosinian orogenesis occurred in Lhasa terrain and the evidence from muscovite $^{40}Ar-^{39}Ar$ geochronology [J]. Acta Petrologica Sinica, 2008, 24: 1595−1604.

[64] Spear F S. Metamorphic Phase Equilibria and Pressure− Temperature− Time Paths [J]. Mineralogical Society of America, Monograph, 1993: 799.

[65] Mahar E M, Baker J M, Powell R, et al. The effect of Mn on mineral stabilityin metapelites [J]. Journal of Metamorphic Geology, 1997, 15: 223−238.

[66] Matsumoto K, Hirajima T. The coexistence of jadeite and omphacite in an eclogite− facies metaquartz diorite from the southern Sesia Zone, Western Alps, Italy [J].Contributions to Mineralogy and Petrology, 2005, 100: 70−84.

[67] Spear F S, Cheney J T. A petrogenetic grid for pelitic schists in the system SiO_2−Al_2O_3−FeO−MgO−K_2O−H_2O [J]. Contributions to Mineralogy and Petrology, 1989, 101: 149−164.

[68] Symmes G H, Ferry J M. The effect of whole−rock Mn−content on the stability of garnet in pelite schists during metamorphism[J]. Journal of Metamorphic Geology, 1992, 10: 221−237.

[69] Tinkham D K, Zuluaga C A, Stowell H H. Metapelite phase equilibria modeling in MnNCKFMASH: the effect of variable Al_2O_3 and MgO/(MgO+FeO) on mineral stability [J]. Geological Materials Research, 2001, 3: 1−42.

[70] Wei Chunjing, Powell R , Clarke G L. Calculated phase equilibria for low− and medium−pressure metapelites in the KFMASH and KMnFMASH systems [J]. Journal of Metamorphic Geology, 2004, 22: 495−508.

[71] Powell R, Holland T J B, Worley B. Calculating phase diagrams involving solid solutions via nonlinear equations, with examples using Thermocalc [J]. Journal of Metamorphic Geology, 1998, 16: 577−588.

[72] Holland T J B, Powell R. An internally consistent themodynamic data set for phase of petrological interest [J]. Journal of Metamorphic Geology, 1998, 16: 309−343.

[73] White R W, Pomroy N E, Powell R. An in− situ metatexite−diatexite transition in upper amphibolite facies rocks from Broken Hill, Australia [J]. Journal of Metamorphic Geology, 2005, 23, 579−602.

[74] Green E C R, Holland T J B, Powell R. An order−disorder model for omphacitic pyroxenes in the system jadeite− diopside− hedenbergite− acmite, with applications to eclogitic rocks [J]. American Mineralogist, 2007,92:1181−1189.

[75] Powell R, Holland T J B. Relating formulations of the thermodynamics of mineral solid solutions: Activity modeling of pyroxenes, amphiboles, and micas [J]. American Mineralogist 1999, 84: 1−14.

[76] Holland T J B, Baker J, Powell R. Mixing properties and activity−composition relationships of chlorites in the system MgO−FeO−Al_2O_3−SiO_2−H_2O [J]. European Journal of Mineralogy,1998,10: 395−406.

[77] Coggon R, Holland T J B. Mixing properties of phengitic micas and revised garnet phengite thermobarometers [J]. Journal of Metamorphic Geology, 2002, 20: 683−696.

[78] Clarke G L, Powell R, Fitsherbert J A. The lawsonite paradox: A comparison of field evidence and mineral equilibria modeling [J]. Journal of Metamorphic Geology, 2006, 24: 716−726.

[79] Guiraud M, Powell R, Rebay G. H_2O in metamorphism and unexpected behaviour in the preservation of metamorphic mineral assemblages [J]. Journal of Metamorphic Geology, 2001,19: 445−454.

[80] Wei Chunjing, Clarke G L. Calculated phase equilibria for MORB compositions: a reappraisal of the metamorphic evolution of lawsonite eclogite [J]. Journal of Metamorphic Geology, 2011,29: 939−952.

[81] Agard P, Labrousse L, Elvevold S, et al. Discovery of Palaeozoic Fe− Mg carpholite in Motalafjella, Svalbard Caledonides: a milestone for subduction−zone gradients [J]. Geology, 2005, 33: 761−764.

[82] Hermann J, Muntener O, Scambelluri M. The importance of serpentinite mylonites for subduction and exhumation of oceanic crust [J].Tectonophysics, 2000, 327: 225−238.

[83] Platt J P. Exhumation of high pressure rocks: a review of concepts and processes [J].Terra Nova, 1993, 5: 119−133.

[84] Rubatto D, Hermann J. Exhumation as fast as subduction[J]? Geology, 2001, 29: 3−6.